







Numerical Analysis of Natural and Forced Convection Cooling for a Photovoltaic Panel Under Variable Weather Conditions

Atheer Raheem Abdullah^{*}, Mohammed Ali Mahmood Hussein^{*}, Mustafa Abdulsalam Mustafa^{*},
Hashim Raed Hashim Al-Sammarraie^{*}

Department of Mechanical Power Techniques Engineering / Refrigeration and Air-Conditioning Branch, Al-Rafidain University, Baghdad 10064, Iraq

Corresponding Author Email: atheer_raheem@ruc.edu.iq

Copyright: ©2026 The authors. This article is published by IETA and is licensed under the CC BY 4.0 license (<http://creativecommons.org/licenses/by/4.0/>).

<https://doi.org/10.18280/ijht.440226>

ABSTRACT

Received: 2 December 2025

Revised: 29 January 2026

Accepted: 6 February 2026

Available online: 30 April 2026

Keywords:

photovoltaic panel, convection, electrical efficiency, temperature

This study presents a comprehensive numerical investigation of the thermal performance of a photovoltaic (PV) panel (BP 585F m-Si PV) under the influence of multiple atmospheric and engineering variables using ANSYS Fluent simulations. The analysis included five main parameters: wind speed ($0.1\text{--}5\text{ m}\cdot\text{s}^{-1}$), solar irradiance ($250\text{--}1000\text{ W}\cdot\text{m}^{-2}$), ambient temperature ($20\text{--}35\text{ }^{\circ}\text{C}$), relative humidity ($0\text{--}75\%$), and PV panel tilt angle ($0\text{--}75^{\circ}$). The results revealed a complex interaction between these factors that determined the thermal behaviour of panels. Wind speed analysis showed a nonlinear inverse relationship, with the transition from natural to forced convection resulting in a $13\text{ }^{\circ}\text{C}$ temperature decrease, reflecting an estimated 5.85% improvement in electrical efficiency. Solar irradiance intensity analysis confirmed its dominant effect as the primary convective driver, with an increase from 500 to $1000\text{ W}\cdot\text{m}^{-2}$ resulting in a nonlinear temperature increase of $24\text{ }^{\circ}\text{C}$, with the highest value ($73\text{ }^{\circ}\text{C}$) recorded under natural convection conditions. The ambient temperature showed a near-linear relationship, with an increase from 20 to $35\text{ }^{\circ}\text{C}$ increasing the photovoltaic panel operating temperature by $13\text{ }^{\circ}\text{C}$, highlighting the increased cooling challenge in hot climates. Relative humidity analysis showed an inverse relationship with PV panel temperature, with humid air (75%) resulting in a $6\text{ }^{\circ}\text{C}$ decrease compared to dry air (0%). This is attributed to the improved thermophysical properties (specific heat capacity and thermal conductivity) of the humid air. Finally, the tilt angle analysis revealed a strong inverse relationship, where increasing the PV panel tilt from horizontal (0°) to near-vertical (75°) resulted in a dramatic thermal reduction of $19\text{ }^{\circ}\text{C}$, equivalent to an efficiency improvement of approximately 8.55%. This was attributed to improved fluid dynamics, as steeper angles disrupted the thermal boundary layer stability and promoted natural convection and turbulence.

1. INTRODUCTION

Solar energy is a clean and environmentally friendly method of generating electrical energy. A solar or photovoltaic cell is a panel made of special materials, such as silicon, which is a semiconductor material that converts sunlight into electricity. Solar panels are installed outdoors to capture sunlight and are therefore affected by various weather factors such as heat, dust, and humidity. One of the most important factors that negatively affects the efficiency of a solar panel is its operating temperature. The efficiency of photovoltaic panels decreases significantly as the temperature increases [1]. High humidity also reduces the efficiency of solar panels and leads to the deterioration of their manufactured materials over time [2].

Many studies have been conducted to improve the operating temperature of solar panels. Merzah et al. [3] conducted research to study the effectiveness of passive cooling strategies using phase change materials. Their goal was to reduce the operating temperature of solar panels. They found that with increasing aluminum oxide, copper oxide, and zinc

oxide concentrations, the temperature decreased and the electrical efficiency increased. They concluded that nanomaterial-added, PCM-based cooling systems have the potential to increase the thermal efficiency of solar panels. Rousseau and Nouri [4] analyzed the effects of many properties of solar module materials on the operating temperature. They found that the density and specific heat capacity were the most important factors that reduced the operating temperature. Natural convection cooling (passive cooling) is a natural cooling process that occurs without the use of a fan. This phenomenon relies entirely on the buoyant forces generated by the differences in air density due to temperature differences. Natural convection has been used in numerous engineering applications [5]. Conversely, forced convection cooling uses an external force, such as a fan or pump. Cuce et al. [6] carried out an experimental study to analyze the effect of passive cooling on the performance parameters of solar cells. They found that, for the same illumination intensity, the power output of the solar cell increased by using fins, which decreased the cell's temperature.

Hudisteanu et al. [7] carried out simulations to investigate the effects of forced convection cooling on a solar cell with and without a heat sink. They also investigated the effects of sink rib dimensions. They confirmed the importance of using heat sinks to decrease the temperature of the cells. Aljumaili and Alaiwi [8] carried out an analysis to study the effect of using a back surface on the temperature of a solar panel. They utilized a phase-change material (RT55 wax) and a heat sink. They could improve the cell efficiency by 3.5%. Popovici et al. [9] confirmed the effectiveness of using a heat sink, even for small heights of the ribs, in reducing the operating temperature of solar panels. They also studied the effects of rib angle on temperature. Caluianu and Băltărețu [10] developed an experimental module to analyze the temperature field of a BP 585 F module mounted at various distances from a roof. They also numerically studied the module. They investigated the effects of the mounting distance of the cell. Finned air-cooled channels enhance the cooling for PV panels as fin thickness increases [11].

The impact of humidity on the performance of solar cells has been investigated experimentally more than numerically. Thombre et al. [12] noted that the effects of relative humidity on solar panels' performance are significant. High humidity can cause surface condensation on PV panels, resulting in reduced solar irradiance absorbed by PV panels, which leads to a temporary loss in power output. Panjwani and Narejo [13] performed an experimental study to analyze the impact of humidity on solar panels. They found that the power output decreased by 10–15% due to humidity. Abbas et al. [14] emphasized the importance of taking into account the effects of solar irradiation, temperature, and humidity when designing and manufacturing solar panels.

The research conducted on solar cells emphasizes the importance of using Ansys tools to analyze and predict the performance of solar cells under specific conditions. Despite the broad understanding of the effect of temperature on solar panels, a significant challenge remains in quantitatively and dynamically predicting the performance of these panels under the influence of a complex combination of changing atmospheric factors, and not just ambient temperature. The PV cell temperature is dependent on several factors, including solar irradiance, ambient air temperature, wind speed, and relative humidity. This complex interaction makes simplified mathematical modeling insufficient for accurate temperature prediction. Therefore, this study investigates the influence of several key factors to determine the optimal conditions for cell operation, which will achieve the highest possible efficiency.

2. THEORETICAL STUDY

The presented numerical model is based on solving a system of fundamental conservation equations (governing equations) that describe heat transfer and airflow around the photovoltaic panel. These equations are derived from the laws of conservation of mass and energy, along with Newton's second law. These equations are the conservation of mass Eq. (1), momentum Eq. (2), and energy Eq. (3), which are respectively as follows.

$$\frac{\partial \rho}{\partial t} + \nabla \cdot (\rho \vec{v}) = 0 \quad (1)$$

$$\frac{\partial}{\partial t} (\rho \vec{v}) + \nabla \cdot (\rho \vec{v} \vec{v}) = -\nabla p + \nabla \cdot (\bar{\tau}) + \rho \vec{g} \quad (2)$$

$$\frac{\partial}{\partial t} (\rho E) + \nabla \cdot (\vec{v}(\rho E + p)) = \nabla \cdot \left(K \nabla T - \sum_j h_j \vec{J}_j + (\bar{\tau} \cdot \vec{v}) \right) + S_h \quad (3)$$

In the previous equations, t is the time, \vec{v} is the velocity, ρ is the density of the air, p is the pressure, \vec{g} is the gravitational acceleration, $\bar{\tau}$ is the viscous stress tensor. E is the total specific energy of the fluid, defined as the sum of the internal and kinetic energy. T is the static temperature, and K is the thermal conductivity. h is the specific enthalpy. J is the flux. S_h is the source.

The term $\rho \vec{g}$ represents buoyancy forces, which are activated in the type of analysis carried out in this study and cannot be neglected. In this context, the source term corresponds to the convection induced by solar radiation on the PV panel surface. The governing equations are nonlinear partial differential equations, which are generally unsolvable by analytical methods. Consequently, numerical methods are employed to solve them. The Finite Volume Method is used to discretize them.

Radiative heat convection on the photovoltaic panel surface is calculated using the following relation:

$$\dot{q}_{solar} = G \times \alpha \quad (4)$$

G represents solar irradiance, and α is the surface absorption of the solar panel. The electrical efficiency for the PV panel is calculated using the standard linear relationship:

$$\eta_{electrical} = \eta_{ref} - \beta(T_{PV} - T_{ref}) \quad (5)$$

$\eta_{electrical}$ is the electrical efficiency at the operating temperature, η_{ref} is the reference efficiency, β is the negative temperature coefficient, T_{PV} is the operating temperature of the panel, and T_{ref} is the reference temperature, which is mostly 25 °C.

3. THE STUDIED SOLAR PANEL

The photovoltaic solar panel BP 585F m-Si PV module [10] is studied. The geometry and characteristics of the module were obtained from the study [15]. The different layers of the PV module are illustrated in Figure 1. The length and width of the PV panel are 1188 mm × 530 mm. The physical properties of the BP 585F PV module layers are mentioned in Table 1.

Table 1. Physical properties of the BP 585F photovoltaic (PV) module layers [10]

| Material | Thickness [mm] | ρ [kg/m ³] | C_p [J/kg·K] | k [W/m·K] |
|-----------------------------------|----------------|-----------------------------|----------------|-------------|
| Low iron glass | 3 | 3000 | 500 | 1.8 |
| Ethylene-vinyl acetate (EVA) film | 1 | 960 | 2090 | 0.35 |
| PV cell | 0.15 | 2330 | 677 | 148 |
| White polyester | 1 | 1200 | 1250 | 0.15 |

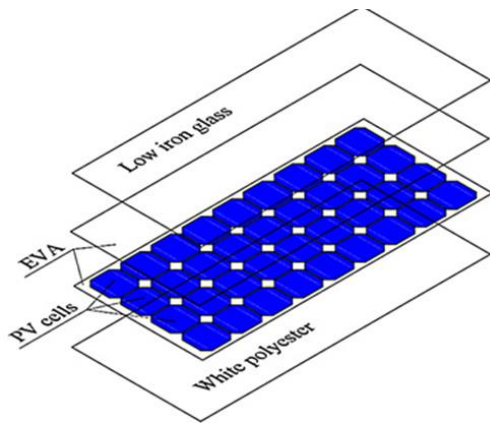


Figure 1. Layers of the BP 585F m-Si PV module [10]

4. NUMERICAL SIMULATION

Three-dimensional simulations were conducted. The PV panel mentioned above was modeled using ANSYS geometry. All layers were represented in the model. A computational domain was then created, as shown in Figure 2. The PV module is positioned in the middle as a solid part. The dimensions of the fluid domain were 6 m upstream of the PV panel, 12 m downstream, and 6 m above and below it. The mesh was constructed by refining the region around the PV panel. A mesh sensitivity analysis was performed to ensure the validity of the numerical results. Figure 3 shows the mesh on the xy-plane. The mesh was refined around the PV panel, which is the most critical region. The PV panel was oriented horizontally in the xz-plane.

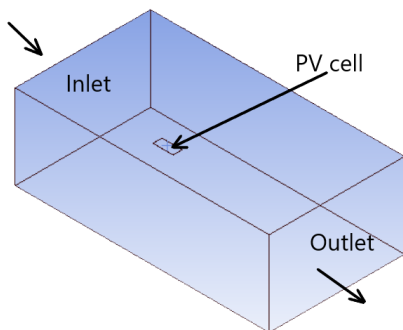


Figure 2. Computation domain with boundary conditions

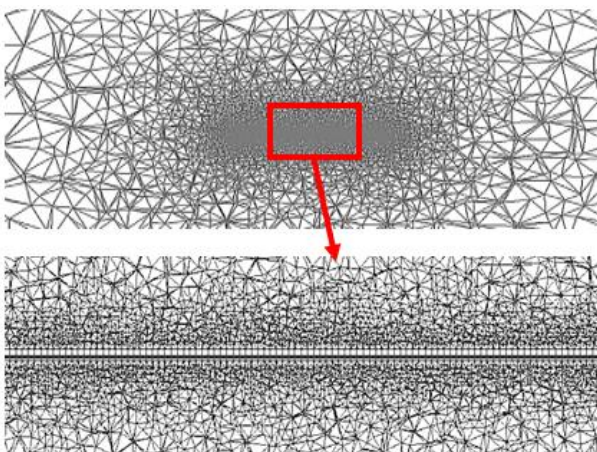


Figure 3. Mesh view in the xy-plane

Steady-state simulations were performed using ANSYS Fluent. The airflow was considered turbulent; thus, the k-epsilon turbulence model was chosen with full buoyancy effects [16]. The properties of the different layers were entered as shown in Table 1. For the mesh sensitivity, a solar radiation intensity of $500 \text{ W}\cdot\text{m}^{-2}$ was applied with $0.5 \text{ m}\cdot\text{s}^{-1}$ inlet velocity. Three meshes were tested with total cell numbers of 674,549, 1,535,485, and 2,765,148. The volume-averaged static temperature of the PV panel layer was compared for the three meshes. The temperatures for the coarse, finer, and finest meshes were 324 K, 317 K, and 316 K, respectively. The difference between the first (coarse) and second (finer) meshes was 6 K. The difference between the second (finer) and the third (finest) meshes was one kelvin. Therefore, the second mesh was selected to perform the simulations. This mesh was the preferred choice for obtaining accurate results within an acceptable computational time.

5. NUMERICAL RESULTS

5.1 Effects of inlet velocity

The first step was to study the effect of wind speed (inlet air velocity) on the PV cell temperature. Several inlet velocities were tested: 0.1, 0.25, 0.5, 1, 2, and $5 \text{ m}\cdot\text{s}^{-1}$. These values were chosen to study the effects of natural and forced convection cooling on the PV cell. The small inlet velocity values ($< 0.5 \text{ m}\cdot\text{s}^{-1}$) represent the natural convection regime, while higher velocities represent forced convection. A solar radiation intensity of $500 \text{ W}\cdot\text{m}^{-2}$ was applied for all inlet velocities. The ambient temperature was set to $25 \text{ }^\circ\text{C}$.

Natural convection cooling depends entirely on buoyancy forces caused by density differences in the air. When a solar panel heats up, it heats the layer of air directly adjacent to it, which then rises. The heated air expands, reducing its density and rising under the influence of buoyancy, and is replaced by cooler, denser air from the surrounding area. This creates natural convection airflow. Natural convection requires no additional power, is simple and reliable, and has no operational costs. However, its effectiveness is limited, particularly on hot, windless days. In the case of forced convection cooling, air is forced to move over the PV panel using an external energy source, such as a fan or pump. In this case, heat transfer is dominated by the inertia of the flow rather than by buoyancy forces. Forced convection is more effective than natural convection, but it requires additional installation and operational costs.

Figure 4 shows the contours of velocity magnitude in the xy-plane for inlet velocities of 0.1, 0.5, and $5 \text{ m}\cdot\text{s}^{-1}$. It can be observed from Figure 4(a) that the velocity contours are irregular. The velocity increases with the inlet velocity owing to the temperature difference between the PV cell and the ambient air. The thickness of the disturbed region around the PV cell is significant. Moreover, the airflow around the PV cell is asymmetric. All these effects are due to natural convection under high temperature differences.

In Figure 4(b), the same effects can be observed, but due to the higher inlet velocity, the airflow irregularity is reduced. However, in Figure 4(c), the airflow is parallel to the PV panel and symmetric, and the thickness of the disturbed region is small compared to that in Figure 4(a). These effects are characteristic of forced convection.

Figure 5 shows the static temperature contours in the xy-

plane for the same inlet velocities as in Figure 4. In Figure 5(a), it can be seen that the thermal boundary layer is thicker than that in Figure 5(b), which in turn is thicker than that in Figure 5(c). The static temperature of the PV cell layer is higher at an inlet velocity of $0.1 \text{ m}\cdot\text{s}^{-1}$ than at $0.5 \text{ m}\cdot\text{s}^{-1}$. The lowest cell temperature occurs at an inlet velocity of $5 \text{ m}\cdot\text{s}^{-1}$. Figure 5 clearly shows the differences between the effects of natural and forced convection.

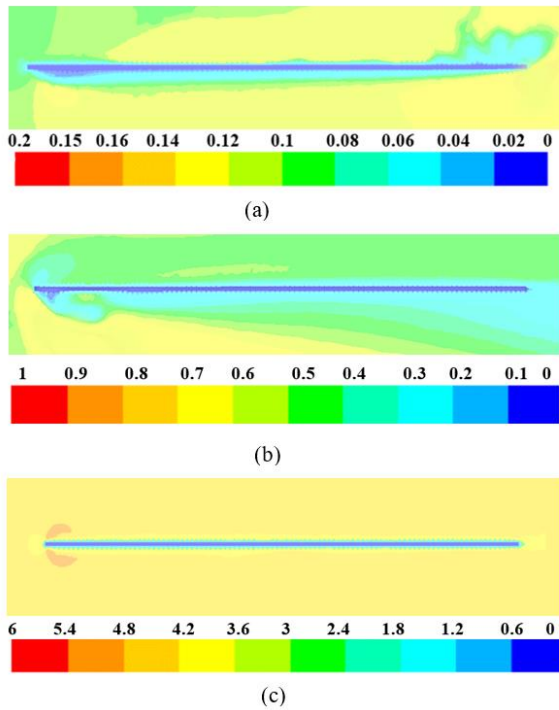


Figure 4. Velocity magnitude contours in xy -plane for inlet velocities: (a) $0.1 \text{ m}\cdot\text{s}^{-1}$; (b) $0.5 \text{ m}\cdot\text{s}^{-1}$; (c) $5 \text{ m}\cdot\text{s}^{-1}$

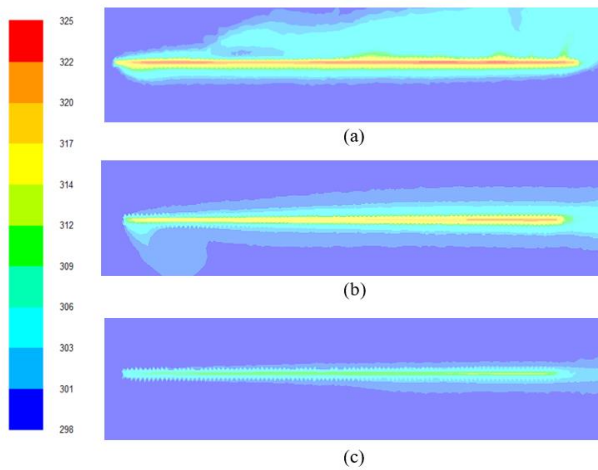


Figure 5. Static temperature contours in xy -plane for different inlet velocities: (a) $0.1 \text{ m}\cdot\text{s}^{-1}$; (b) $0.5 \text{ m}\cdot\text{s}^{-1}$; (c) $5 \text{ m}\cdot\text{s}^{-1}$

Figure 6 shows the thermal boundary layers for the three inlet velocities. The layer with $0.1 \text{ m}\cdot\text{s}^{-1}$ inlet velocity is the thickest. At all three inlet velocities, the temperature near the PV cell changes sharply. The large thickness of the thermal boundary layer hinders the heat exchange between the PV cell and the ambient air.

Figure 7 shows the variation of the PV cell static

temperature with the five chosen inlet velocities. It can be observed that the PV cell temperature decreases sharply when the inlet velocity increases from $0.1 \text{ m}\cdot\text{s}^{-1}$ to $0.5 \text{ m}\cdot\text{s}^{-1}$ ($\Delta T = 5 \text{ }^\circ\text{C}$). An inlet velocity of $0.5 \text{ m}\cdot\text{s}^{-1}$ represents the transition from the natural to forced convection. The temperature of the PV cell continues to decrease as the inlet velocity increases. Higher inlet velocities enhance the heat transfer from the PV cell surface to the ambient air. However, it is noted that the PV cell temperature decreases by $4 \text{ }^\circ\text{C}$ when the inlet velocity increases from $0.5 \text{ m}\cdot\text{s}^{-1}$ to $2 \text{ m}\cdot\text{s}^{-1}$. A similar temperature decrease occurs when the inlet velocity increases from $2 \text{ m}\cdot\text{s}^{-1}$ to $5 \text{ m}\cdot\text{s}^{-1}$.

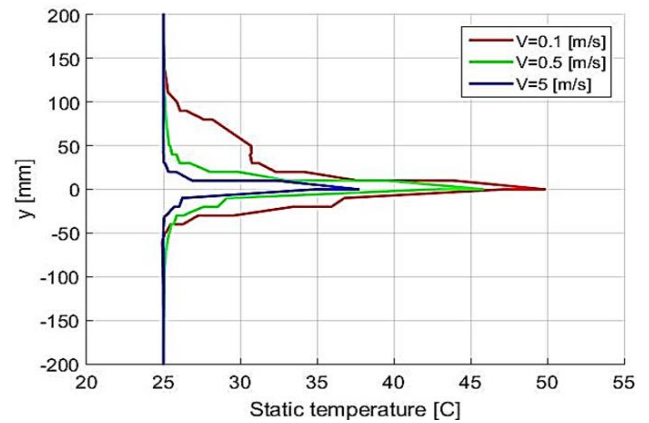


Figure 6. Thermal boundary layer for the same inlet velocities as in Figure 4 and Figure 5

The values of the convective heat transfer coefficient were obtained from ANSYS Fluent for the external surface of the PV cell. The values are $8.0, 8.5, 9.1, 9.2, 10.2,$ and $12.3 \text{ W}\cdot\text{m}^{-2}\cdot\text{K}^{-1}$ for inlet velocities of $0.1, 0.25, 0.5, 1, 2,$ and $5 \text{ m}\cdot\text{s}^{-1}$, respectively. These results indicate that increasing the inlet velocity increases the convective cooling efficiency. The coefficient starts with a value of $8.0 \text{ W}\cdot\text{m}^{-2}\cdot\text{K}^{-1}$ (with $0.1 \text{ m}\cdot\text{s}^{-1}$), and it increases slightly with low inlet velocities ($0.25, 0.5,$ and $1 \text{ m}\cdot\text{s}^{-1}$). Then, it jumps to $12.3 \text{ W}\cdot\text{m}^{-2}\cdot\text{K}^{-1}$ with the inlet velocity $5 \text{ m}\cdot\text{s}^{-1}$. Increasing the inlet velocity increases the airflow over the solar panel, which enhances the convective cooling process between the PV cell and the ambient air. Furthermore, this increase in the convective heat transfer coefficient from 8.0 to $12.3 \text{ W}\cdot\text{m}^{-2}\cdot\text{K}^{-1}$ corresponds to an improvement in cooling efficiency of approximately 54% .

The electrical efficiency of a solar panel is a key parameter for evaluating its performance. The relative electrical efficiency was calculated according to Eq. (5):

$$\eta_{\text{improvement}} = \beta \times \Delta T$$

where, $\beta = 0.0045$ for a silicon base cell, and ΔT is the temperature difference between the PV cell temperature and the reference temperature, which is $25 \text{ }^\circ\text{C}$. Calculating the relative efficiency at an inlet velocity of $5 \text{ m}\cdot\text{s}^{-1}$ compared to $0.1 \text{ m}\cdot\text{s}^{-1}$ shows an improvement of approximately 5.8% .

It can be concluded from the results presented above that windy days are better for cooling the PV cell. However, on days with still air, the temperature of the PV cell increases, and natural convection cooling is insufficient. Moreover, beyond a certain wind speed, one cannot rely on the wind alone to cool the PV cell.

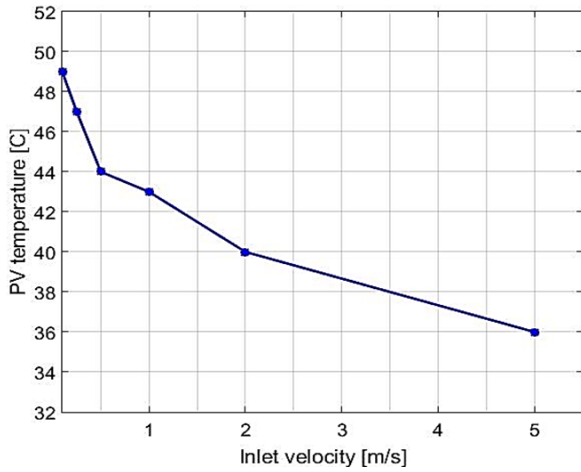


Figure 7. Variation of photovoltaic (PV) cell static temperature with inlet velocity

5.2 Effects of solar irradiance and ambient temperature

Multiple parameters affect the relationship between solar irradiance and ambient temperature [17, 18]. The main parameters are air humidity, wind speed, PV panel position, and cloud cover. Moreover, several modules exist for estimating the relationship between solar irradiance and ambient temperature [19, 20]. In this study, four solar irradiance values were selected: 250, 500, 750, and 1000 $\text{W}\cdot\text{m}^{-2}$, while the ambient temperature was fixed at 25 $^{\circ}\text{C}$. The inlet velocity for these simulations was set to 0.1 $\text{m}\cdot\text{s}^{-1}$. This inlet velocity was chosen to isolate the effects of solar irradiance. The volume-averaged static temperature of the PV cell was recorded for each case.

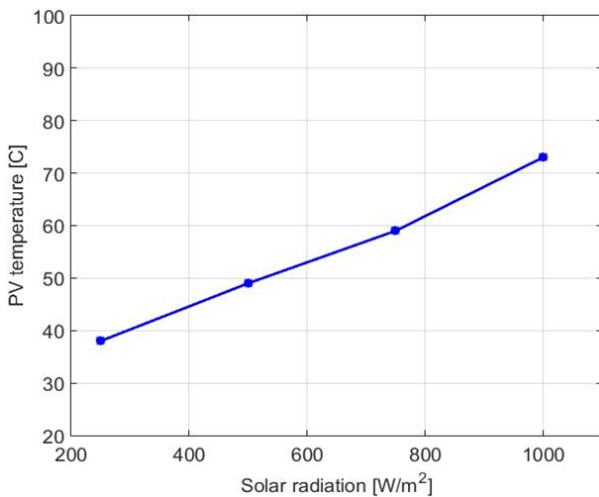


Figure 8. Variation of photovoltaic (PV) cell static temperature with solar irradiance

Figure 8 shows the variation of the static temperature of the PV cell with solar irradiance. It is evident that the PV cell temperature increases with irradiance. The results reveal a nonlinear relationship between irradiance and temperature rise. Although doubling the irradiance from 500 to 1000 $\text{W}\cdot\text{m}^{-2}$ approximately doubles the incoming power, the corresponding temperature increases (from 49 $^{\circ}\text{C}$ to 73 $^{\circ}\text{C}$, a 24 $^{\circ}\text{C}$ rise) are more than twice the increase observed when irradiance was doubled from 250 to 500 $\text{W}\cdot\text{m}^{-2}$ (11 $^{\circ}\text{C}$ rise). This behaviour can be explained by the Stefan–Boltzmann law of thermal

radiation, where the rate of heat loss by radiation from a surface $q_{rad} = \varepsilon\sigma(T_{surface}^4 - T_{ambient}^4)$ is proportional to the fourth power of the absolute temperature. Natural convection cooling is insufficient to manage the heating from high solar irradiance. This indicates that forced convection cooling is more effective under conditions of high solar irradiance.

Second, the solar irradiance was fixed at 500 $\text{W}\cdot\text{m}^{-2}$, and the ambient temperature was varied from 20 to 35 $^{\circ}\text{C}$. Figure 9 shows the variation in the PV cell static temperature with ambient temperature. As shown in Figure 9, the relationship between the ambient temperature and the PV cell temperature is linear. This indicates that a change in ambient temperature results in an approximately equal change in the PV cell temperature. Therefore, the difference between the PV cell temperature and the reference temperature increases in hot climates. The efficiency loss is about 9% at 20 $^{\circ}\text{C}$ and about 15% at 35 $^{\circ}\text{C}$.

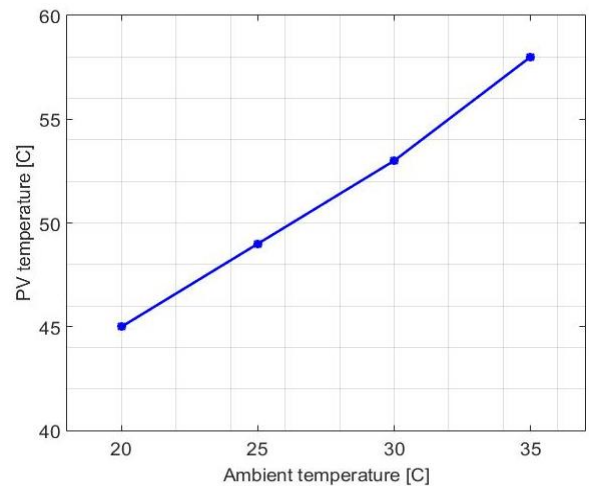


Figure 9. Variation of photovoltaic (PV) cell static temperature with ambient temperature

5.3 Effect of air humidity

Natural and forced convection are affected by air humidity. The properties of air, such as density, viscosity, thermal conductivity, and specific heat capacity, vary depending on whether the air is dry or humid. Therefore, the temperature of a PV cell differs from its temperature in dry or humid air. To test the effects of humidity in this study, the solar irradiance was fixed at 500 $\text{W}\cdot\text{m}^{-2}$, the ambient temperature at 25 $^{\circ}\text{C}$, and the inlet velocity at 0.1 $\text{m}\cdot\text{s}^{-1}$. Relative humidity was set to 0%, 25%, 50%, and 75%.

Figure 10 shows the static temperature of the PV cell for different levels of relative humidity. It can be observed that a low level of humidity (25%) has a negligible effect, reducing the PV cell temperature by only 1 $^{\circ}\text{C}$ compared to dry air. However, at a relative humidity of 50%, the PV cell temperature decreases by 5 $^{\circ}\text{C}$. This can be attributed to the increase in the thermal conductivity and specific heat capacity of air with rising humidity, which enhances convective heat transfer. By increasing the relative humidity to 75%, the PV cell temperature decreases by only 1 $^{\circ}\text{C}$. However, certain effects cannot be investigated with this type of numerical simulation. Humidity deteriorates the PV cell materials. The accumulation of moisture on the cell surface reduces convective cooling and reflects sunlight, resulting in less power output.

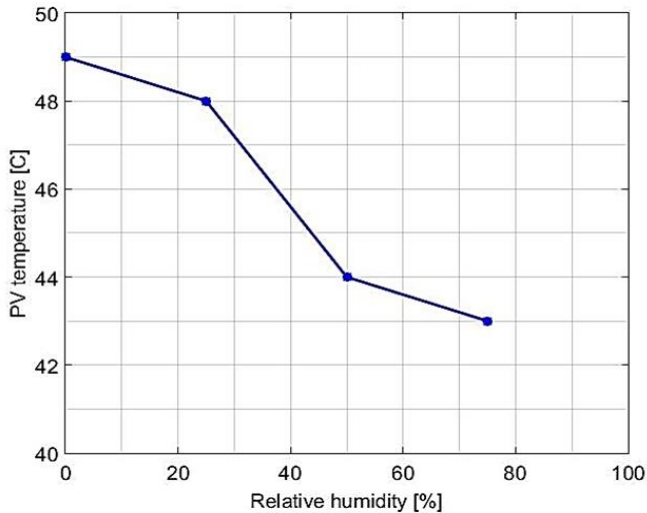


Figure 10. Variation of photovoltaic (PV) cell static temperature with relative humidity

5.4 Effect of photovoltaic panel tilt angle

The angle of the PV cell relative to a horizontal surface, as shown in Figure 11, was investigated. This is the tilt angle. It affects both the received solar irradiance and convective cooling.

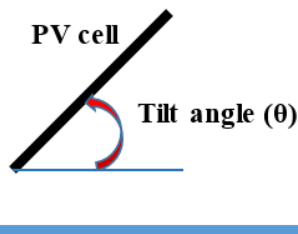


Figure 11. Schematic of the photovoltaic (PV) panel tilt angle

Simulations were performed with a solar irradiance of $500 \text{ W}\cdot\text{m}^{-2}$ and an inlet velocity of $0.1 \text{ m}\cdot\text{s}^{-1}$. The volume-averaged temperature of the PV cell is shown in Figure 12. The Figure shows that increasing the tilt angle decreases the PV cell temperature. The effectiveness of natural convection is low at small tilt angles and increases with angle; this is because the convective airflow becomes stronger and more effective. Quantitative analysis of the results shows that the temperature follows a decreasing trend with increasing tilt angle. The reduction in PV cell temperature was most pronounced when moving from low to moderate tilt angles (a $14 \text{ }^\circ\text{C}$ decrease from 0° to 60°), and more gradual at higher angles (an additional $5 \text{ }^\circ\text{C}$ decrease from 60° to 75°). This suggests a saturation point, where the cooling benefit of increasing the tilt angle becomes limited, possibly due to geometric factors that reduce the interaction between the panel surface and the horizontal airflow. However, increasing the tilt angle reduces the intensity of incident solar irradiance.

The tilt angle is an important parameter. It has to be set according to climate conditions. In hot and dry climates, high irradiance and high ambient temperatures are expected. These conditions increase the operating temperature of the PV cell. A high tilt angle (e.g., 60°) is recommended; reducing the

operating temperature of the PV cell is more important than the received irradiance, which is expected to be high. In temperate climates, maximizing the received irradiance and minimizing the operating temperature of the PV cell is not easy. For year-round operating, a tilt angle of around 15° may be recommended. In cold climates, maximizing the received irradiance is the most important factor. A near-zero tilt angle is recommended.

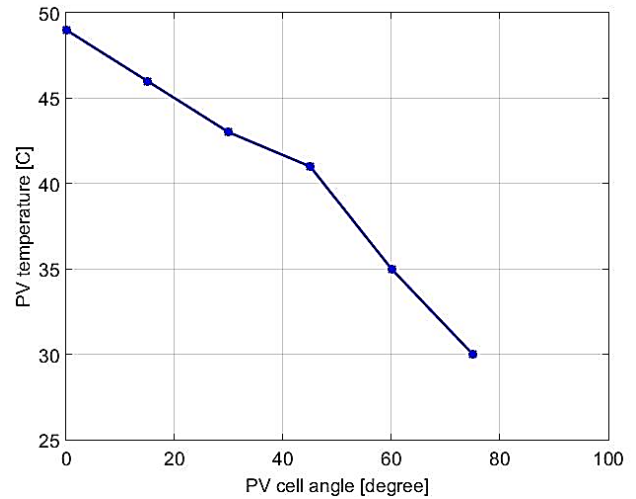


Figure 12. Variation of photovoltaic (PV) cell static temperature with tilt angle

In conclusion, the tilt angle is a critical factor. The optimal tilt angle cannot be given easily, even for a specific location. An adjustable mounting system is the best choice. It permits changing the tilt angle according to ambient conditions, which may change daily.

6. IMPLICATIONS FOR DESIGN AND COOLING STRATEGIES

The presented results can be used as a base to suggest cooling systems, which can improve the thermal performance of photovoltaic panels. Two types of cooling systems can be suggested.

- 1- Hybrid cooling systems: Analyzing the relation between the wind speed and the PV cell temperature showed a nonlinear curve (Figure 7). Moreover, it exists a point (a small wind speed) where the convective cooling is ineffective. Therefore, a hybrid cooling system can be recommended. It is supplied with fans, which are switched on when the wind speed is low ($< 0.5 \text{ m}\cdot\text{s}^{-1}$). When the wind speed exceeds a certain value ($\geq 2 \text{ m}\cdot\text{s}^{-1}$), the fans are switched off for energy savings. Using such a hybrid system can ensure the effectiveness of convective cooling. Therefore, maximizing the efficiency of solar panels. The presented results gave these selected points numerically.
- 2- Passive evaporative cooling: The presented results showed that air humidity is a positive parameter in cooling solar panels. In hot and dry climates, solar panels can be supplied with a porous back cover when the cover is moistened with water. It evaporates, which cools the air adjacent to the back of the panel. The presented results showed the effectiveness of this

idea. Harnessing humidity for cooling solar panels is an energy-saving method of cooling.

7. CONCLUSIONS

This study presents an analysis of the thermal performance of a photovoltaic panel under the influence of five environmental and design parameters. Three-dimensional numerical simulations were carried out to study the effects of the selected parameters, which are wind speed, solar irradiance, ambient temperature, relative humidity, and tilt angle. The effect of each parameter has been studied and analyzed individually. Synthesizing the relationships between the effects of each parameter can help draw applicable optimization strategies.

First, a multifactor coupling analysis reveals nonlinear interactions that determine design priorities:

- The effects of irradiance and ambient temperature are compounded, as their combined increase drives the system toward critical operating conditions.
- The effect of wind speed is most significant when a high thermal load exists (high irradiance and high ambient temperature), while its benefit is marginal under moderate conditions.
- Humidity acts as a beneficial modifier that mitigates the severity of temperature rise.

Second, based on an implicit cost-benefit analysis of the studied factors, the following guidelines for engineering practice are recommended:

- Highest priority (low cost, high impact): Optimizing the tilt angle during the initial design phase is the most feasible intervention, requiring minimal additional investment beyond the initial study.
- Medium priority (medium cost, high impact): In regions with high irradiance and low wind speeds, simple hybrid cooling systems can be considered, where low-consumption fans operate only when the panel temperature exceeds a set point, and the natural wind speed is below an effective threshold (less than approximately $0.5 \text{ m}\cdot\text{s}^{-1}$, as shown in this study).
- Important priority for future development (higher cost/complexity): Developing materials or backsheets with moisture-wicking properties can transform high atmospheric humidity from a constraint into a performance-enhancing feature, especially in coastal regions.

REFERENCES

- [1] Skoplaki, E., Palyvos, J.A. (2009). On the temperature dependence of photovoltaic module electrical performance: A review of efficiency/power correlations. *Solar Energy*, 83(5): 614-624. <https://doi.org/10.1016/j.solener.2008.10.008>
- [2] Tripathi, A.K., Ray, S., Arunav, M., Prasad, S. (2021). Evaluation of solar PV panel performance under humid atmosphere. *Materials Today: Proceedings*, 45(7): 5916-5920. <https://doi.org/10.1016/j.matpr.2020.08.775>
- [3] Merzah, B.N., Almakhyoul, Z.M., Abdullah, A.R., Ayed, S.K., Majdi, H.S. (2024). Enhancing solar panel cooling and thermal efficiency using nanoparticle-enhanced phase change materials. *Mathematical Modelling of Engineering Problems*, 11(6): 1547-1557. <https://doi.org/10.18280/mmep.110615>
- [4] Rousseau, P., Nouri, H. (2023). Ansys investigation of solar photovoltaic temperature distribution for improved efficiency. *International Journal of Advances in Applied Sciences*, 12(3): 293-300. <http://doi.org/10.11591/ijaas.v12.i3.pp293-300>
- [5] Mahmood, M.A., Mustafa, M.A., Al-Azzawi, M.M., Abdullah, A.R. (2024). Natural convection heat transfer in a concentric annulus vertical cylinders embedded with porous media. *Journal of Advanced Research in Fluid Mechanics and Thermal Sciences*, 66(2): 65-83.
- [6] Cuce, E., Bali, T., Sekucoglu, S.A. (2011). Effects of passive cooling on performance of silicon photovoltaic cells. *International Journal of Low-Carbon Technologies*, 6(4): 299-308. <https://doi.org/10.1093/ijlct/ctr018>
- [7] Hudisteanu, S., Mateescu, T.D., Chereches, N.C., Popovici, C.G. (2012). Numerical study of air cooling photovoltaic panels using heat sinks. *Revista Romana de Inginerie Civila*, 6(1): 1-20.
- [8] Aljumaili, A.T., Alaiwi, Y. (2023). Enhancement of the polycrystalline solar panel performance using a heatsink cooling system with PCM. *International Journal of Engineering and Artificial Intelligence*, 4(1): 24-34. <https://doi.org/10.55923/jo.ijea.4.1.103>
- [9] Popovici, C.G., Hudişteanu, S.V., Mateescu, T.D., Cherecheş, N.C. (2016). Efficiency improvement of photovoltaic panels by using air cooled heat sinks. *Energy Procedia*, 85: 425-432. <https://doi.org/10.1016/j.egypro.2015.12.223>
- [10] Caluianu, I.R., Băltăreţu, F. (2012). Thermal modelling of a photovoltaic module under variable free convection conditions. *Applied Thermal Engineering*, 33-34: 86-91. <https://doi.org/10.1016/j.applthermaleng.2011.09.016>
- [11] Zheng, Y., Miao, J., Yu, H., Liu, F., Cai, Q. (2023). Thermal analysis of air-cooled channels of different sizes in naturally ventilated photovoltaic wall panels. *Buildings*, 13(12): 3002. <https://doi.org/10.3390/buildings13123002>
- [12] Thombre, J., Kulkarni, A., Gadgil, B. (2025). Effect of temperature and relative humidity on PV cell for electricity generation – A review. *International Research Journal of Modernization in Engineering Technology and Science*, 7(6).
- [13] Panjwani, M.K., Narejo, G.B. (2014). Effect of humidity on the efficiency of solar cell (photovoltaic). *International Journal of Engineering Research and General Science* 2(4): 499-503. <https://oaji.net/articles/2014/786-1406207313.pdf>
- [14] Abbas, Z., Harijan, K., Shaikh, P.H., Walasai, G.D., Ali, F. (2020). Effect of ambient temperature and relative humidity on solar PV system performance: A case study of Quaid-e-Azam solar park, Pakistan. *Sindh University Research Journal*, 49(004): 721-726. <http://doi.org/10.26692/sujo/2017.12.0047>
- [15] BP 585F m-Si PV Module Technical Information, 2002. <https://www.bpsolar.com>, accessed on Jan. 2, 2025.
- [16] Bardina, J.E., Huang, P.G., Coakley, T.J. (1997). Turbulence modeling validation, testing, and development. NASA Technical Memorandum 110446.
- [17] Morteza-pour, H., Ghobadian, B., Khoshtaghaza, M.H., Minaee, S. (2012). Performance analysis of a two-way hybrid photovoltaic/thermal solar collector. *Journal of Agricultural Science and Technology*, 14: 767-780.

[18] Khatib, T., Mohamed, A., Mahmoud, M., Sopian, K. (2011). Modeling of daily solar energy on a horizontal surface for five main sites in Malaysia. *International Journal of Green Energy*, 8(8): 795-819. <http://doi.org/10.1080/15435075.2011.602156>

[19] Kabré, A., Bonkoungou, D., Koalaga, Z. (2024). Analysis of the effect of temperature and relative humidity on the reliability of a photovoltaic module. *Advances in Materials Physics and Chemistry*, 14(8): 165-177. <https://doi.org/10.4236/ampc.2024.148013>

[20] Dubey, S., Sarvaiya, J.N., Seshadri, B. (2013). Temperature dependent photovoltaic (PV) efficiency and its effect on PV production in the world – A review. *Energy Procedia*, 33: 311-321. <https://doi.org/10.1016/j.egypro.2013.05.072>

| | |
|---|---|
| p | pressure, $N \cdot m^{-2}$ |
| q | radiative heat convection, $W \cdot m^{-2}$ |
| S | source, $W \cdot m^{-3}$ |
| t | time, s |
| T | temperature, K |
| v | velocity, $m \cdot s^{-1}$ |

Greek symbols

| | |
|------------|--|
| ρ | density, $kg \cdot m^{-3}$ |
| τ | stress tensor |
| α | surface absorption |
| η | photovoltaic efficiency |
| β | energy temperature coefficient, K^{-1} |
| ϵ | emissivity |
| σ | Stefan–Boltzmann constant, $W \cdot m^{-2} \cdot K^{-4}$ |

NOMENCLATURE

| | |
|---|--|
| c | specific heat capacity, $J \cdot kg^{-1} \cdot K^{-1}$ |
| E | total specific energy, $J \cdot kg^{-1}$ |
| g | gravitational acceleration, $m \cdot s^{-2}$ |
| G | solar irradiance, $W \cdot m^{-2}$ |
| h | specific enthalpy, $J \cdot kg^{-1}$ |
| J | flux, $kg \cdot m^{-2} \cdot s^{-1}$ |
| k | thermal conductivity, $W \cdot m^{-1} \cdot K^{-1}$ |

Subscripts

| | |
|-----|-------------------|
| j | in j-direction |
| ref | reference |
| PV | photovoltaic |
| p | constant pressure |
| h | enthalpy |